PHYSICAL REVIEW B **87**, 081301(R) (2013)

Electron transfer in hydrogenated nanocrystalline silicon observed by time-resolved terahertz spectroscopy

Matthew R. Bergren,[1,4] Brian J. Simonds,[1] Baojie Yan,[2] Guozhen Yue,[2] Richard Ahrenkiel,[3,4] Thomas E. Furtak,[1] Reuben T. Collins,[1] P. Craig Taylor,[1] and Matthew C. Beard[4]

[1]*Department of Physics, Colorado School of Mines, Golden, Colorado 80401, USA*

[2]*United Solar Ovonic, Auburn Hills, Michigan 48326, USA*

[3]*Metallurgical and Materials Engineering Department, Colorado School of Mines, Golden, Colorado 80401, USA*

[4]*National Renewable Energy Laboratory, Golden, Colorado 80401, USA*

(Received 5 November 2012; revised manuscript received 17 December 2012; published 4 February 2013)

We report on the ultrafast carrier dynamics in hydrogenated nanocrystalline silicon (nc-Si:H) using time-resolved terahertz spectroscopy. Photoexcitation at 407 nm primarily produces charge carriers in the *a*-Si phase, but they undergo a rapid electron transfer to the *c*-Si phase prior to complete thermalization into the band-tail states of *a*-Si. We studied the carrier dynamics on a range of nc-Si:H samples with varying crystalline volume fractions (X_c) and mapped out the carrier dynamics with sub-ps resolution. Our measurements are consistent with a model in which electrons are first trapped at interface states at the *a*-Si–*c*-Si boundary prior to being thermally emitted into the *c*-Si phase. Wavelength and temperature dependent measurements are consistent with our model. The phenomena observed here have implications toward solar cell structures that utilize an amorphous material as an absorber layer, previously thought to have a mobility value too low to attain effective charge transport in a device.

DOI: 10.1103/PhysRevB.87.081301 PACS number(s): 73.63.−b, 72.20.Jv, 72.80.−r, 78.47.D−

Hydrogenated nanocrystalline silicon (nc-Si:H) is an emerging thin-film photovoltaic material[1,2] that combines advantages of silicon (*c*-Si), like high carrier mobility, with less expensive production methods of amorphous silicon (*a*-Si). One major advantage is the reduction of light-induced degradation prevalent in *a*-Si.[3–5] The nc-Si:H films studied here differ from microcrystalline silicon (μc-Si) and are comprised of monodisperse and nonaggregated prolate spheroid-shaped silicon nanocrystals (NCs), with a 20 nm long axis and a 6-nm diameter, embedded in an *a*-Si matrix.[6,7] Recently, photoluminescence (PL) quenching and light induced electron spin resonance (LESR) experiments suggest that charge carriers photoexcited into *a*-Si undergo rapid electron transfer (ET) to the NCs prior to thermalization into the band-tail states of *a*-Si.[8] In this report, we employ ultrafast time-resolved terahertz spectroscopy (TRTS) to directly monitor these dynamics.

A schematic of the proposed kinetics is shown in Fig. 1. Incident photons with energy greater than ∼1.7 eV excite electrons primarily in *a*-Si (1-a), with a smaller fraction excited directly in the NCs (1-c). A large fraction of those carriers produced in *a*-Si are rapidly trapped at *c*-Si–*a*-Si interfaces (2a) prior to thermalization (2a'). Carriers trapped at interfaces are thermally injected into the conduction band (CB) of *c*-Si (3) and establish a dynamic equilibrium, as carriers undergo many trapping and detrapping events prior to eventual recombination (4). In device applications, carriers undergo percolative transport, and the trapping and detrapping events lead to dispersive transport behavior.[9] Evidence for the proposed model is obtained with PL and LESR experiments,[8] which are low-temperature, steady-state measurements. They show that as the X_c increases above 0.2 the PL from *a*-Si is increasingly quenched and replaced by an interface defect PL band at lower energies, where at $X_c = 0.75$ all PL results from interface defects. Since carriers thermalize to band-tail states in ∼1 ps,[10–12] hot-carrier transfer must be faster.

In this paper, TRTS is employed to directly observe the ultrafast carrier dynamics and probe the ET kinetics discussed above. TRTS has sub-ps to ns resolution and is most sensitive to mobile charge carriers, such as carriers in the extended states of amorphous semiconductors, whose absorption cross sections at THz frequencies are directly proportional to the carrier mobility. Any carriers that have been trapped in the material will not contribute to the THz signal.

The nc-Si:H films were deposited by a plasma-enhanced chemical vapor deposition process, in which silane was diluted with hydrogen to encourage NC nucleation. In contrast to μc-Si deposition, the hydrogen dilution was dynamically varied to attain monodisperse NCs throughout the film.[7] The X_c was varied by changing the hydrogen-silane ratio and confirmed with Raman spectroscopy.[13] All films were approximately 1-μm thick, deposited on glass (Corning 7059).

TRTS is a pump-probe experiment that measures the photomodulated differential THz electric field, $\Delta E/E = (E_{\text{on}} - E_{\text{off}})/E_{\text{off}}$, where $E_{\text{on/off}}$ is the transmitted THz field with the 407-nm (3.05-eV) excitation pulses on (unblocked) and off (blocked). Our TRTS experimental apparatus is described elsewhere,[14] and reviews of TRTS experiments for measuring carrier dynamics can be found in the literature.[15,16] For small values of $\Delta E/E$ (<0.1), the effective photoconductivity for a thin-film semiconductor can be obtained through[17,18]

$$\left|\frac{-\Delta E(\tau_p)}{E}\right| = \frac{\Delta\sigma_{\text{eff}}(\tau_p)\cdot z}{(1+n_s)c\varepsilon_0} = \frac{e\cdot z}{(1+n_s)c\varepsilon_0}[X_a n_a(\tau_p)\mu_a + X_c n_c(\tau_p)\mu_c], \quad (1)$$

where n_s is the refractive index of substrate at THz frequencies ($n_s = 1.95$), c is the speed of light, τ_p is the time delay between the pump and probe pulses, and ε_0 is the free-space permittivity. The effective photoconductivity $\Delta\sigma_{\text{eff}}$ is expressed as the weighted sum of the conductivities in

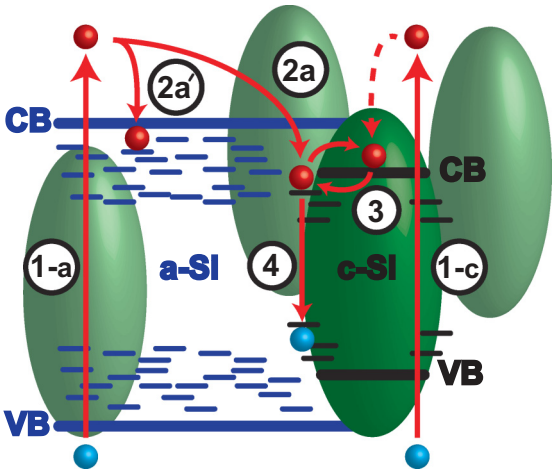

FIG. 1. (Color online) Schematic of the ET process. In steps 1-a and 1-c, light produces carriers in *a*-Si or *c*-Si. Hot carriers in *a*-Si are trapped at the *a*-Si–*c*-Si interface (2a) or cool into the band-tail states (2a'). Trapped electrons establish a thermal equilibrium with carriers in the CB of the nanocrystals. Finally, electrons eventually recombine (4).

a-Si and *c*-Si, where e is the charge of an electron; n_a,n_c are the electron densities in each phase; μ_a,μ_c are their respective mobilities; and X_c,X_a are their respective volume fractions. Since TRTS is proportional to the charge-carrier mobility, trapped carriers, with low mobility, do not contribute. Similarly, carriers that reach the band-tail states of *a*-Si do not contribute appreciably. The photoexcited path length z is the optical absorption depth ($1/\alpha_{\text{eff}}$), where α_{eff} is the effective absorption coefficient and is assumed to be a weighted linear summation: $\alpha_{\text{eff}} = X_c\alpha_c + (1 - X_c)\alpha_a$. Literature values for α_a and α_c at 407 nm were taken from Refs. 19 and 20 to be $\alpha_c^{407} = 9.52 \times 10^4\ \text{cm}^{-1}$ and $\alpha_a^{407} = 5.24 \times 10^5\ \text{cm}^{-1}$. For these studies, z varies between 0.08 and 0.15 μm (at 407 nm), such that incident light is either reflected or absorbed.

Implicit in Eq. (1) is the assumption that electrons are the dominant charge carriers contributing to the TRTS response. For carriers in the *a*-Si region, this is validated by the large difference between electron and hole mobilities of ~3 orders of magnitude.[21] However, in bulk *c*-Si, the ratio of the two mobilities is ~2.5,[22] which we consider a lower bound for the NCs. The scattering length in bulk *c*-Si is much larger than the dimensions of the NC, such that carriers in the crystallite interact with surfaces. The localized valence-band-tail (VBT) states are associated with bonding states that are more strongly affected by variations in bond lengths and angles than the conduction-band-tail (CBT) states. This pushes the VBT states deeper into the band gap than the CBT states, resulting in more localized hole wave functions.[23] Since these band tails exponentially decrease into the band gap, this localization further reduces the hole mobility from the bulk *c*-Si value. Therefore, we neglect contributions to the carrier dynamics from the hole.

The THz response normalized by the absorbed fluence represents a weighted sum of mobilities,[24] and Eq. (1)) can be written as $|-\Delta E(\tau_p)/E| \cdot (1 + n_s) \cdot c \cdot \varepsilon_0/(e \cdot J_{\text{abs}}) = \Delta\sigma_{\text{eff}}(\tau_p) \cdot z/(e \cdot J_{\text{abs}}) = f_a(\tau_p)\mu_a + f_c(\tau_p)\mu_c$, where $f_{a,c}$ is the fraction of the total number of carriers in the *a*-Si or *c*-Si phases at delay time τ_p, and $J_{\text{abs}} = (1 - R) \cdot J_0$, where R is the reflection coefficient ($R = 0.47$). Room-temperature TRTS data, plotted as $\Delta\sigma_{\text{eff}}(\tau_p) \cdot z/(e \cdot J_{\text{abs}})$, are shown in Figs. 2(a)–2(c) for X_c values of 0.7, 0.5, 0.3, 0.2, and *a*-Si. The 407-nm excitation pulse had an input fluence J_0 of 3.4×10^{14} photons/cm^2 for 0.5 and 0.3, while $J_0 = 5 \times 10^{14}$ photons/cm^2 for the 0.7, 0.2 samples, and *a*-Si. The initial rise is governed by the convolution of the system response function (SRF) and the optical absorption, which partitions carriers into the *a*-Si–*c*-Si regions. At the peak of the initial THz response, $\tau_p = 0$, $\Delta\sigma_{\text{eff}}(\tau_p = 0) \cdot z/(e \cdot J_{\text{abs}}) = f_a(0)\,\mu_a + f_c(0)\,\mu_c$, where $f_c(0) = X_c\alpha_c/\alpha_{\text{eff}}$, is the fraction of light absorbed in *c*-Si, and $f_a(0) = 1 - f_c(0)$. The fast decay of the signal from 0–5 ps results from carriers initially excited into the *a*-Si phase and either thermalized to the band tail or underwent ET to interface states (see 2a and 2a' in Fig. 1). To quantify the intrinsic decay time within *a*-Si, we modeled the THz response of *a*-Si (black circles and line) as a single exponential decay convoluted with a Gaussian SRF (full width at half maximum ~0.5 ps), and we find that $\tau_{a-\text{Si}} = 2.1$ ps, consistent with previous TRTS[25] and transient absorption measurements.[10,12] At $\tau_p = 5$ ps, all carriers initially excited into *a*-Si no longer contribute and $\Delta\sigma_{\text{eff}}(\tau_p \cong 5\text{ps}) \cdot z/(e \cdot J_{\text{abs}}) = f_c(0)\,\mu_c$. From the response at $\tau_p = 0$ and 5 ps, we can determine both μ_a and μ_c and find $\mu_a = 3.0$, 1.8, and 2.5 cm^2 V^{-1} s^{-1}, while $\mu_c = 21$, 44, and 33 cm^2 V^{-1} s^{-1} for 0.7, 0.5, and 0.3 samples, respectively. The variations in μ_a and μ_c across the three samples likely occur from differences in NC size, *a*-Si quality, and defect density. The *a*-Si mobility values are reasonable when compared with the value of ~4.5 cm^2 V^{-1} s^{-1} reported by Lui and Hegmann.[25] The THz measurement probes the mobility of carriers in *a*-Si prior to their thermalization and is higher than typically reported values measured with a dc probe, because carriers in the dc case interact with shallow defect states on longer time scales.[25] In contrast, μ_c is more than an order of magnitude lower than typical values for bulk silicon, with $\mu_{\text{bulk}}^{c-\text{Si}} \sim 1300$ cm^{2}V^{-1}s^{-1}. Smaller mobilities found here can be understood by considering the mean-free path l_f of carriers in bulk Si compared to the NC dimensions. l_f is on the order of ~160 nm, eight times larger than the NC dimensions. We estimate the effect of grain boundaries on μ_c by calculating a modified mean-free path, $1/l_{\text{eff}} = 1/l_f + 1/a$, where a denotes the NC dimensions (taken here to be 20 nm). Therefore, the mobility should be reduced to 60–100 cm^2 V^{-1} s^{-1} due to this effect. The values reported here are lower than this, indicating that other things such as defects and variations in NC geometry could be affecting the transport properties of *c*-Si in these films.

The THz signal partially recovers in ~200 ps for the 0.3, 0.5, and 0.7 samples as carriers trapped at interface states are released into *c*-Si, while no recovery is observed in the *a*-Si or 0.2 case. The recovery of the signal provides direct evidence that some fraction of the carriers that originated in the *a*-Si reach the interface states rather than thermally relaxing to the *a*-Si band-tail states. This observation is consistent with PL quenching and LESR experiments.[8] No appreciable recovery is observed for the 0.2 sample, suggesting that carriers excited into *a*-Si thermalize prior to reaching the NC boundary in that case.

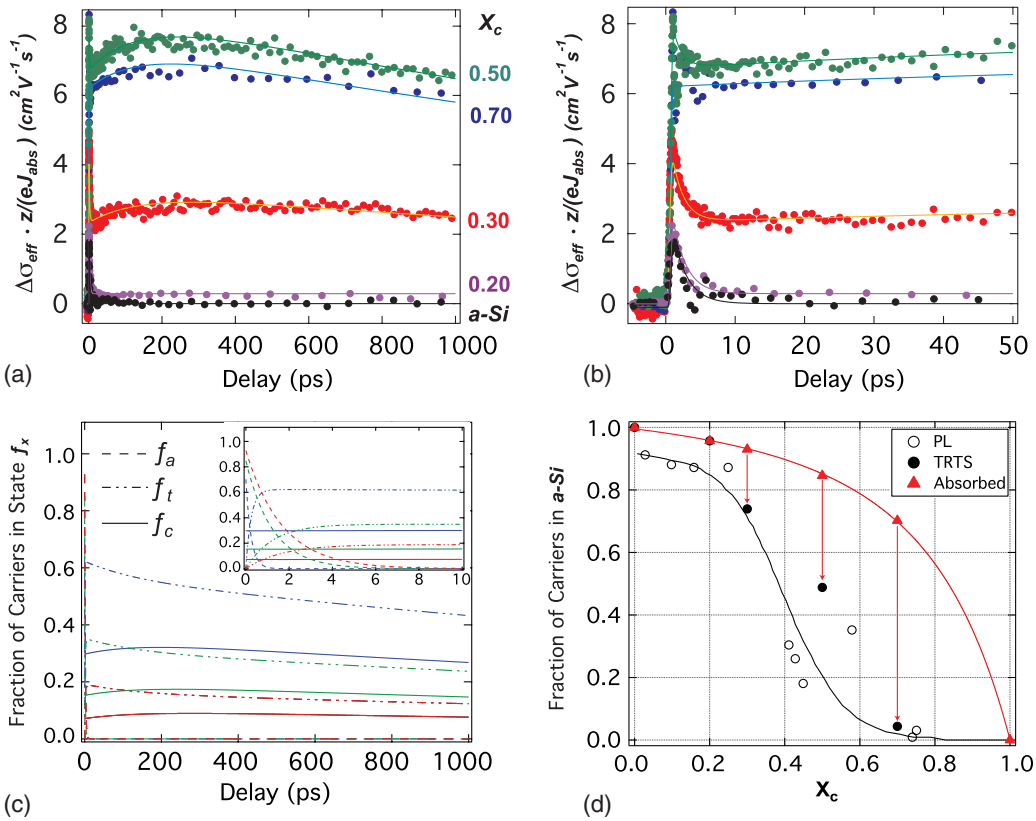

FIG. 2. (Color online) (a) 300 K TRTS transient data for X_c varying from 0 (a-Si) to 0.7. (b) TRTS data at early delay times. Solid lines represent a linear least-squares best fit of our model (see text) to the data. (c) The fraction of carriers in each state in our model as a function of delay. Inset: early time behavior. (d) The fraction of the total carriers remaining in a-Si calculated from this study (black circles) and PL data from Ref. 8. Red triangles represent the fraction of total photons absorbed in a-Si.

To model the TRTS data, we consider the time-dependent population of three states: the a-Si extended state f_a, the interface trap state f_t, and the c-Si extended state f_c. The dynamics are parameterized by four time constants, representing the initial transfer of excited electrons to the interface traps, τ_1 (2a); the thermal emission of trapped carriers to the c-Si, τ_2 (3); the trapping of carriers from the c-Si, τ_3 (3); and a recombination rate, τ_4 (4). In our model, we don't differentiate between recombination from interface or extended states, and both are probably occurring in these films. The thermalization time $\tau_{a-\mathrm{Si}}$ (2a') in a-Si is fixed at the value determined above. The rate equations governing the populations of carriers in these states are

$$\begin{aligned}\frac{df_a}{dt} &= -\frac{f_a(t)}{\tau_1} - \frac{f_a(t)}{\tau_{a-\mathrm{Si}}},\\ \frac{df_t}{dt} &= \frac{f_a(t)}{\tau_1} - \frac{f_t(t)}{\tau_2} + \frac{f_c(t)}{\tau_3} - \frac{f_t(t)}{\tau_4},\\ \frac{df_c}{dt} &= \frac{f_t(t)}{\tau_2} - \frac{f_c(t)}{\tau_3}.\end{aligned} \tag{2}$$

This system of equations was solved numerically for f_a, f_t, and f_c, with the following initial conditions: $f_a(0) = X_a\alpha_a/\alpha_{\mathrm{eff}}$, $f_t(0) = 0$, and $f_c(0) = X_c\alpha_c/\alpha_{\mathrm{eff}}$. We assumed that at 407 nm excitation the carriers were absorbed in crystalline and amorphous phases according to α_c and α_a, their respective absorption coefficients. $f_c(t)$ and $f_a(t)$ were convolved with the SRF described above $G(t - t_0)$. The data were modeled by $G(t - t_0) \otimes [\mu_a f_a(t) + \mu_c f_c(t)]$, where $\otimes$ represents a convolution. We performed a global linear least-squares fit to the 0.7, 0.5, and 0.3 data, allowing τ_1 to vary for each trace, while τ_2, τ_3, and τ_4 were global variables. The values of μ_a, μ_c, and $\tau_{a-\mathrm{Si}}$ are held fixed at the values determined above. The results for the best-fit parameters are summarized in Table I.

Figure 2(c) shows the dynamics for each state. At early times, carriers reside in either a-Si or c-Si. Carriers in a-Si quickly transfer to interface states and then emit into the c-Si phase. The fraction of initial carriers excited into a-Si phase that reach the a-Si–c-Si boundary is greatest for the 0.7 sample, can be determined by $\tau_1^{-1}/(\tau_1^{-1} + \tau_{a-\mathrm{Si}}^{-1})$, and is 0.9, 0.4, and 0.2 for the 0.7, 0.5, and 0.3 samples, respectively. In Fig. 2(d) we compare the fraction of carriers remaining in the a-Si phase as a function of X_c determined in this study (closed circles) with that determined via PL quenching experiments (open circles). The fraction of photons that are directly absorbed into the a-Si phase is shown with red triangles. The difference between the red triangles and the closed circles (shown by the red arrow) represents carriers that undergo fast injection into the interface states. This difference increases with X_c.

Excitation at 815 nm (1.52 eV) preferentially excites carriers into the c-Si phase (by a factor of ~20), whereas 407 nm (3.05-eV) excitation preferentially excites into a-Si [see Fig. 3(a)]. However, α_c is two orders of magnitude smaller ($\alpha_c^{407} = 9.52 \times 10^4$ cm^{-1}, $\alpha_c^{815} = 274$ cm^{-1}), resulting in a

TABLE I. Best-fit parameters for data in Fig. 2.

X_c	τ_1 (ps)	τ_{a-Si} (ps)	τ_2 (ps)	τ_3 (ps)	τ_4 (ps)	μ_a (cm^2 V^{-1} s^{-1})	μ_c (cm^2 V^{-1} s^{-1})
0.7	0.14 (0.05)					2.5[a]	33[a]
0.5	3.0 (0.4)	2.1[a]	361 (2)	211 (19)	2292 (244)	1.8[a]	44[a]
0.3	8.1 (0.7)					3.0[a]	21[a]

[a]Parameters were held constant during fitting, with one standard deviation error in parentheses. Values in the shaded box represent global variables.

lower overall J_{abs} such that not all of the photons are absorbed in the 1-μm thick film. To compensate, J_0 was increased to 3.7×10^{15} photons/cm^2 so that the total number of photons absorbed in the c-Si phase is approximately equal to that at $\lambda_{ex} = 407$ nm. Thus $\Delta\sigma_{eff}(\tau_p) \cdot z/(e \cdot J_{abs})$ at $\sim$5 ps in the 407-nm data is equal to the 815-nm data peak, because this represents carriers directly absorbed by c-Si. The data from the 815-nm excitation reveal an additional complexity. Even though the numbers of carriers absorbed by the two phases are approximately equal, the number of carriers per NC in c-Si varies by an order of magnitude because photons are absorbed within 0.1 μm at 407 nm but absorbed in 1 μm at 815 nm. We also verified that the dynamics are insensitive to J_0 for both 815-nm and 407-nm excitation over one order of magnitude (data not shown). Photothermal deflection spectroscopy (PDS) was used to measure the total absorption coefficient α_{tot} of the 0.5 film, and it shows that linearly adding α_a and α_c at 815 nm underestimates α_{tot} [see inset in Figs. 3(a)]. In fact, α_{tot} is higher in the 0.5 film than either α_a or α_c. This indicates that states not associated with either a-Si or c-Si absorb $\sim$50% of the total absorbed light. We speculate that this is caused by interface states that are directly excited by the pump beam. The model was, therefore, adjusted, by changing the initial conditions above to be $f_a(0) = (1 - f_c)$, $f_t(0) = f_c \cdot f'$, and $f_c(0) = f_c \cdot (1 - f')$, where f' is the fraction of photons directly absorbed into interface states with 815-nm excitation. Our final global linear least-squares fit included the 815-nm data set and converged on a value of 0.57 for f'. At 407 nm, excitation into the defect states is minimal compared to the absorption by a-Si and c-Si.

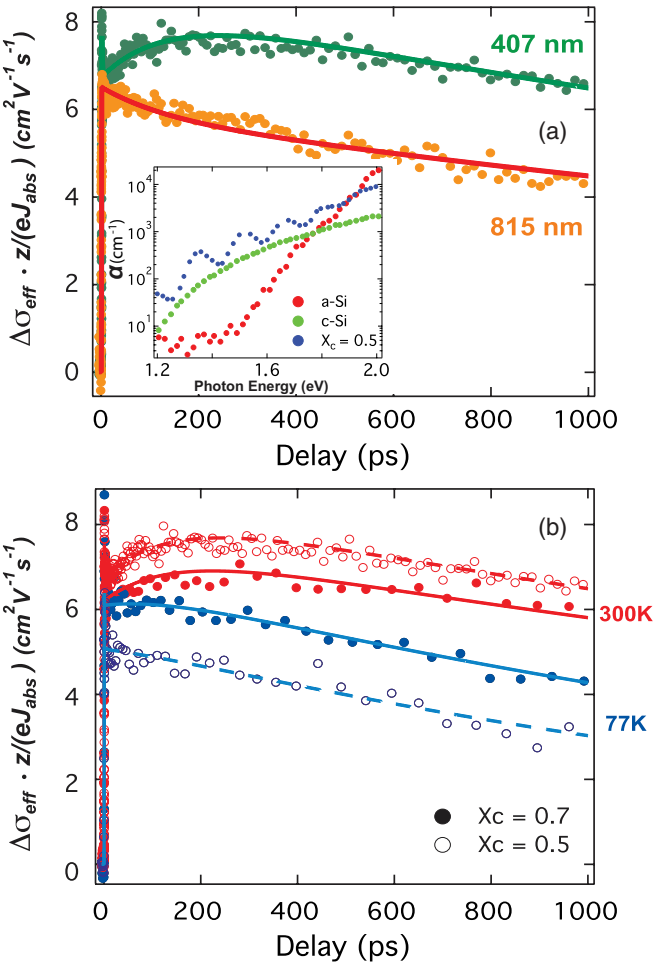

FIG. 3. (Color online) (a) Wavelength dependence of the carrier dynamics at 300 K for the $X_c = 0.5$ sample for 407 and 815 nm excitation. Inset: PDS measurements of the absorption coefficient of a-Si:H, $X_c = 0.5$ nc-Si:H, and literature data for c-Si.[19] (b) 300 and 77 K data for the $X_c = 0.7$ and 0.5 samples and their linear squares best fits (solid, 0.7; dashed, 0.5).

In Fig. 3(b) we compare the 407-nm dynamics for the $X_c = 0.7$ and 0.5 films at 300 and 77 K. Unlike at 300 K, the 77-K data show little to no signal recovery after the carriers in a-Si are trapped. The recovery is absent at low temperature because the trap emission process is thermally activated, and the number of electrons that can participate decreases with temperature. We preformed a linear least-squares fit of our model to the 77-K data, where most parameters were set equal to those used in the analysis of the 300-K data. Only the lifetimes τ_2, τ_4 were allowed to vary. The values of μ_c^{77K} and μ_a^{77K} extracted for the $X_c = 0.5$ and 0.7 samples were 4.8 and 81 cm^2 V^{-1} s^{-1} and 8.6 and 51 cm^2 V^{-1} s^{-1}, respectively. At 77 K, μ_a^{77K} increased slightly, while μ_c^{77K} remained the same or decreased. The best-fit values for τ_2 increased to 447 ps for the 0.7 sample and 501 ps for the 0.5 sample, while τ_4 decreased by $\sim$1 ns. This supports the hypothesis that fewer electrons participate in thermal emission into the extended states of c-Si at low temperature.

In conclusion, we have directly observed electron transfer in nc-Si:H films using time-resolved terahertz spectroscopy and have proposed a trap-mediated model that accurately describes the data. The model shows that a fraction of electrons excited in a-Si become trapped at the a-Si–c-Si interface before they can thermalize to the a-Si band-tail states and then thermally inject into the nanocrystal. These results demonstrate that charge transfer out of amorphous materials can be achieved, which suggests the use of solar cells where photons can be absorbed in the amorphous phase and charges can be transported by a more

conductive material. It also has implications toward using an amorphous matrix in hot-carrier solar cells, since the electron transfer could occur faster than the thermalization process.

ACKNOWLEDGMENTS

This material is based upon work supported by the NSF through the Renewable Energy Materials Research Science and Engineering Center under Grant No. DMR-0820518. Terahertz measurements performed at the National Renewable Energy Laboratory (NREL) were supported by the Center for Advanced Solar Photophysics, an Energy Frontier Research Center funded by the US Department of Energy (DOE), Office of Science, Office of Basic Energy Sciences. DOE funding was provided to the NREL through Contract No. DE-AC36-08G028308.

[1] B. Yan, G. Yue, X. Xu, J. Yang, and S. Guha, Phys. Status Solidi A **207**, 671 (2010).
[2] S. Hazra and S. Ray, Solid State Commun. **109**, 125 (1998).
[3] G. Yue, B. Yan, G. Ganguly, J. Yang, and S. Guha, J. Mater. Res. **22**, 1128 (2007).
[4] S. Guha, J. Yang, D. L. Williamson, Y. Lubianiker, J. D. Cohen, and A. H. Mahan, Appl. Phys. Lett. **74**, 1860 (1999).
[5] T. Kamei, P. Stradins, and A. Matsuda, Appl. Phys. Lett. **74**, 1707 (1999).
[6] K. G. Kiriluk, D. L. Williamson, P. C. Taylor, B. Yan, G. Yue, J. Yang, and S. Guha, J. Non-Cryst. Solids **357**, 2587 (2011).
[7] B. Yan, G. Yue, Y. Yan, C.-S. Jiang, C. W. Teplin, J. Yang, and S. Guha, *Materials Research Society Symposium Proceedings* 1066 (Cambridge University Press, Cambridge, England, 2008).
[8] K. G. Kiriluk, J. E. Fields, B. J. Simonds, Y. P. Pai, P. L. Miller, T. Su, B. Yan, J. Yang, S. Guha, A. Madan, S. E. Shaheen, P. C. Taylor, and R. T. Collins [Appl. Phys. Lett. (2013) (to be published)].
[9] B. J. Simonds, B. Yan, G. Yue, and R. K. Ahrenkiel, and P. C. Taylor, *Photovoltaic Specialists Conference (PVSC) 35th IEEE* 2010 (IEEE, New York, NY, 2010).
[10] M. Wraback and J. Tauc, Phys. Rev. Lett. **69**, 3682 (1992).
[11] P. M. Fauchet, D. Hulin, R. Vanderhaghen, A. Mourchid, and W. L. Nighan, J. Non-Cryst. Solids **141**, 76 (1992).
[12] J. O. White, S. Cuzeau, D. Hulin, and R. Vanderhaghen, J. Appl. Phys. **84**, 4984 (1998).
[13] E. Bustarret, M. A. Hachicha, and M. Brunel, Appl. Phys. Lett. **52**, 1675 (1988).
[14] J. E. Murphy, M. C. Beard, and A. J. Nozik, J. Phys. Chem. B **110**, 25455 (2006).
[15] M. C. Beard, G. M. Turner, and G. M. Schmuttenmaer, J. Phys. Chem. B **106**, 7146 (2002).
[16] M. Ulbricht, E. Hendry, J. Shan, T. F. Heinz, and M. Bonn, Rev. Mod. Phys. **83**, 543 (2011).
[17] J. I. Pankove, *Optical Process in Semiconductors* (Dover, Englewood Cliffs, 1971).
[18] P. Kuzel, F. Kadlec, and H. Nemec, J. Chem. Phys. **127**, 024506 (2007).
[19] D. E. Aspnes, *Properties of Crystalline Silicon* (INSPEC, London, 1999).
[20] G. D. Cody, in *Semiconductors and Semimetals*, edited by J. I. Pankove, Vol. 21 (Academic, Orlando, 1984).
[21] R. A. Street, *Hydrogenated Amorphous Silicon*, Cambridge Solid State Science Series (Cambridge University Press, Cambridge, 1991).
[22] S. H. Jones, *Properties of Crystalline Silicon* (INSPEC, London, 1999).
[23] K. Morigaki, *Physics of Amorphous Semiconductors* (Imperial College Press, London, 1999).
[24] L. Fekete, P. Kuzel, H. Nemec, F. Kadlec, A. Dejneka, J. Stuchlik, and A. Fejfar, Phys. Rev. B **79**, 115306 (2009).
[25] K. P. H. Lui and F. A. Hegmann, J. Appl. Phys. **93**, 9012 (2003).